

Resonant X-ray Scattering Study of Magnetic Ordering in SmNi_2Ge_2

Z. Islam,^{1,2} J. C. Lang,² L. Vasiliu-Doloc,^{1,2} G. Srajer,² P. C. Canfield³

¹ Department of Physics, Northern Illinois University, DeKalb, IL, U.S.A.

² Advanced Photon Source, Argonne National Laboratory, Argonne, IL, U.S.A.

³ Ames Laboratory and Dept. of Physics and Astronomy, Iowa State University, Ames, IA, U.S.A.

Introduction

In a recent study, generalized electronic susceptibility calculations using the tight-binding linear-muffin-tin-orbital electronic bands, found pronounced nesting between two bands with strong $5d$ character at the Fermi level in the RNi_2Ge_2 series of materials (14/mmm). It was shown that this nesting is responsible for the single incommensurate magnetic modulation vector of the form $\mathbf{q}=(0\ 0\ q_z)$, with q_z in the range 0.75-0.81 r.l.u., observed in the tripositive R members of the series.¹ The primary objective of the present study was to investigate the magnetic structures of the Sm members of the series to see if they are consistent with the Fermi-surface nesting picture. To our knowledge, no definitive work on the magnetic structures exists. X-ray resonant exchange scattering (XRES)² provides an ideal tool for studying this structure, since Sm is opaque to neutrons and the inherently high- Q resolution of XRES is ideal for incommensurate structures. The high-quality single crystal of SmNi_2Ge_2 used in this work was grown by a high-temperature solution-growth technique at Ames Laboratory.³ This material orders antiferromagnetically at $T_N = 17.9$ K and exhibits planar anisotropy above T_N . Two additional transitions at lower temperatures below T_N are also observed, at $T_1 = 11.8$ K and $T_2 = 5.5$ K, respectively.⁴ Due to the minimum obtainable temperature of 8.0 K, in this work we were primarily concerned with the ordered phases above T_2 .

Experimental Details

The XRES studies were performed on the bending magnet beamline in sector 1 of SRI CAT.5 A Si (111) reflection was used to monochromatize the beam, which was then focused both vertically and horizontally down to a spot size of $600\ \mu\text{m} - 700\ \mu\text{m}$, respectively, at the sample. Higher harmonic contaminations in the beam were eliminated by using two Pd-coated mirrors. A rec-

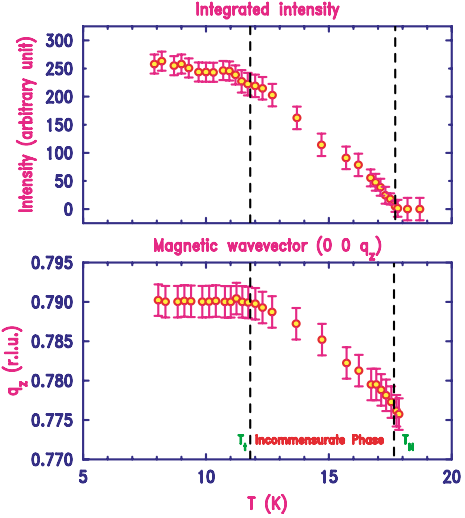


FIG. 2. Temperature dependence of the magnetic peak.

tangular sample with dimensions $2.5 \times 0.9 \times 0.3\ \text{mm}^3$ was aligned with the $[H\ 0\ L]$ zone in the vertical scattering plane. The sample was oriented, cut, and polished perpendicular to $[0\ 0\ 1]$. The mis-cut angle was $\sim 5^\circ$. The mosaic was 0.05° . Initially, the incident photon energy was tuned to the L_{II} edge (7.312 keV) of Sm in order to use the resonant enhancement. The $(0\ 0\ 6)$ reflection from a flat pyrolytic graphite crystal was used as the polarization analyzer. The integrated intensity was measured using a Ge solid-state detector. The sample was sealed in a Be can with He exchange gas and cooled in a closed-cycle He refrigerator.

Results

According to the nesting picture, the magnetic modulation vector is expected to lie along \mathbf{c}^* , with a q_z value in the range mentioned above. A reciprocal lattice scan, at 8.0 K, revealed superlattice peaks corresponding to $(0, 0, 0.79)$. Figure 1 (left panel) shows an energy scan through the satellite peak at $(0, 0, 4.79)$. There is a strong resonance that occurs a few eV above the absorption edge, at 7.314 keV, with an enhancement factor of ~ 35 relative to the background ~ 25 eV below the edge. Polarization analysis (Fig. 1. right panel) revealed that the incident linear polarization perpendicular to the scattering plane (σ polarization) is completely rotated into the scattering plane (π polarization). The resonance and polarization properties are consistent with a magnetic origin of the superlattice peak.^{2,6} At 12.0 K, just

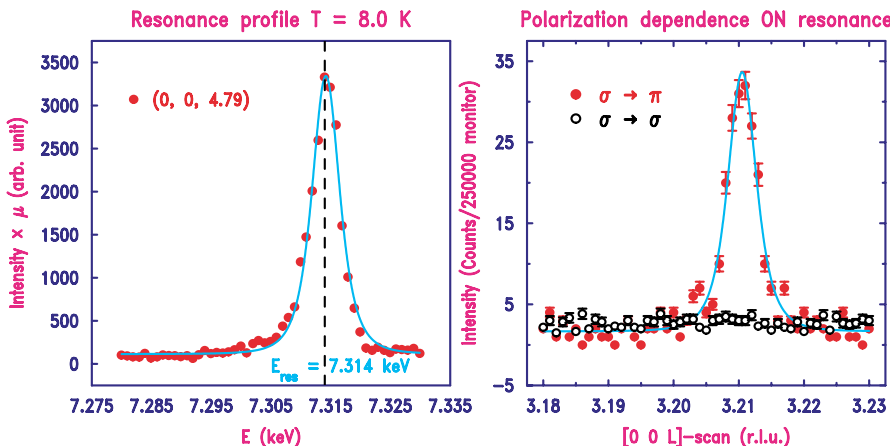


FIG. 1. Left panel: Energy scan through Sm L_{II} edge of a superlattice peak. Right panel: Polarization analysis.

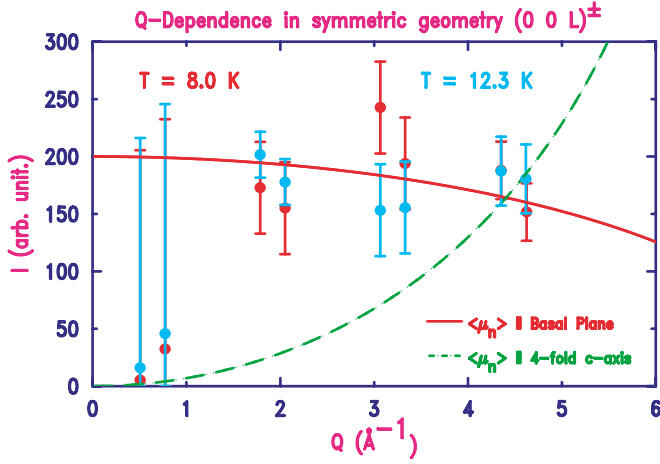


FIG. 3. Q -dependence of magnetic satellites.

above T_i but below T_N , a similar scan found the magnetic satellite with a small change in position and diminished intensity. No third harmonics were observed indicating the absence of squaring-up of these phases.

Figure 2 summarizes the temperature dependence of the ordered phases. The integrated intensity of the magnetic peak (top panel) remains nearly temperature independent below T_i , suggesting saturation of the ordered Sm moments. Above T_i , the intensity decreases monotonically and disappears above T_N . The lower panel shows the variation of the magnetic modulation with T . In the phase below T_N but above T_i , the modulation vector changes continuously with T approaching ~ 0.775 r.l.u., indicating the incommensurate nature of the ordering, consistent with the Fermi-surface nesting picture. Below T_i , however, the structure is characterized by a temperature-independent $\mathbf{q} = (0, 0, 0.79 \pm 0.002)$, suggesting a long-period ordered phase. T_i is identified as the temperature at which q_z reaches this value with a concomitant near saturation of the intensity, which is 11.8 ± 0.2 K.

In order to ascertain the direction of the ordered moments the trend in the intensity of magnetic peaks was measured as a function of Q . As can be seen in Fig. 3, with the exception of the two low- Q data points, in both phases the data (solid circles) can be modeled well with model calculations assuming that the ordered moments are in the basal plane (solid line). Similar trends in the Q -dependence were observed for Eu and Gd nickel germanides in their low-temperature phases with the moments locked in the

basal plane.¹ On the other hand, the model with the moments along the c -axis is manifestly in disagreement with the data. The apparent order-of-magnitude reduction of the intensities at very low Q is due to sample miscut (see above).

Conclusions

In summary, the primary result of this work is that the magnetic structures of the Sm-member of the $R\text{Ni}_2\text{Ge}_2$ series conform to the topological nesting of the Fermi surface. SmNi_2Ge_2 orders in an incommensurate antiferromagnetic structure characterized by a single propagation vector, $\mathbf{q}=(0\ 0\ q_z)$. The value of q_z is T dependent and approaches ~ 0.775 r.l.u. near $T_N = 17.8 \pm 0.2$ K. No evidence of squaring-up of this structure was observed. In both the ordered phases above T_i the ordered moments are confined to the basal plane, as in the case of a basal-plane helical or a plane wave.

Acknowledgment

We would like to thank J. Pollmann for his help during the initial set up of the experiment, and D. Haskel, D. Wermeille, and S. K. Sinha for stimulating discussions on rare-earth magnetism, magnetic resonance and related phenomena. Use of the Advanced Photon Source is supported by the U.S. Department of Energy, Office of Science, Office of Basic Energy Sciences, under Contract No. W-31-109-ENG-38. Part of this work is supported by the State of Illinois under HECA. Ames Laboratory (DOE) is operated by Iowa State University under Contract No. W-7405-Eng-82.

References

- ¹ Z. Islam, C. Detlefs, C. Song, A.I. Goldman, V. Antropov, B.N. Harmon, S.L. Bud'ko, T. Wiener, P.C. Canfield, D. Wermeille, K.D. Finkelstein, Phys. Rev. Lett. **83**, 2817 (1999); Z. Islam, Ph. D. Thesis, Iowa State University (1999).
- ² J.P. Hannon, G.T. Trammell, M. Blume, and D. Gibbs, Phys. Rev. Lett. **61**, 1245 (1988); D. Gibbs, D.R. Harshman, E.D. Isaacs, D.B. McWhan, D. Mills, and C. Vettier, Phys. Rev. Lett. **61**, 1241 (1988).
- ³ P.C. Canfield, and Z. Fisk, Phil. Mag. B **56**, 1117 (1992).
- ⁴ S.L. Bud'ko, Z. Islam, T.A. Wiener, I.R. Fisher, A.H. Lacerda, P.C. Canfield, J. Magn. Magn. Mat. **205**, 53 (1999).
- ⁵ J.C. Lang, G. Srajer, J. Wang, and P.L. Lee, Rev. Sci. Instrum. **70**, 4457 (1999).
- ⁶ J.P. Hill and D.F. McMorrow, Acta. Crystallogr. Sec. A **5**, 236 (1996).